

Quantum-state reconstruction in the one-atom maser

C. T. Bodendorf,^{1,2} G. Antesberger,^{1,2} M. S. Kim,^{1,*} and H. Walther^{1,2}

¹Max-Planck-Institut für Quantenoptik, Hans-Kopfermann-Strasse 1, Garching, D-85748, Germany

²Sektion Physik, Ludwig-Maximilians-Universität, München, Germany

(Received 14 August 1997)

We propose a reconstruction scheme for the quantum-mechanical state of a field inside a microwave cavity in the Fock representation. It will be shown that two experimental steps are required for this purpose: (i) the quantum state under consideration has to be shifted in phase space, and (ii) it has to be examined by state-selective detection of two-level atoms after a resonant interaction with the field. The method is examined in a computer simulation including measurement errors. [S1050-2947(98)04802-1]

PACS number(s): 42.50.Dv, 42.50.Ct, 84.40.Ik

I. INTRODUCTION

In quantum mechanics all physical properties of a system are contained in the state vector; once it is known, the maximum information that quantum mechanics allows us to gain is at hand. However, the state itself is *not* a measurable quantity. Nevertheless it is possible to “reconstruct” a quantum state based on a suitable set of measurements. This topic has been discussed extensively in recent years [1–11].

There are always at least two prerequisites associated with a reconstruction: The first one concerns the preparation of the system under investigation. To gain sufficient information about the quantum state, it has to be prepared not only once but rather frequently in a reproducible way. The second prerequisite is a set of linearly independent Hermitian operators for which expectation values can be determined by measurements. Each set contains a certain amount of information about the quantum state and therefore fixes a so-called “*observation level*” [2]. The *complete observation level*, containing the full information on any arbitrary state, requires in many cases an *infinite* number of observables. For this reason it is in practice often inevitable to restrict oneself to a *partial* reconstruction.

A partial reconstruction of a quantum state has been performed through its quasiprobabilities [3]. The density matrix for the squeezed vacuum has also been partially reconstructed in Fock representation [4]. These reconstruction schemes of light field states are based on the homodyne measurement. It has recently been suggested that the direct photon statistics can also serve as a tool to probe the field state [5–8].

In this paper we deal with the single-mode microwave field inside a high- Q cavity, which shall be the system under investigation. However, this system itself evades a direct observation because of the lack of single microwave photon detectors, and, moreover, the destruction of the required extremely high quality factor, which would be the consequence of any attempt at a direct field measurement. But fortunately there exists a much more adequate procedure via the detection of atoms after their interaction with the field mode.

Two-level atoms are resonantly coupled to a single mode of the cavity. Before the interaction the atoms are prepared in one of the two levels. The subsequent temporal evolution of the combined atom-field system is—because of the cavity damping time for a typical experimental situation being three orders of magnitude larger than the interaction time—an almost *reversible* process, described by the Jaynes-Cummings model [12]. After the interaction the atoms are detected by state-selective field-ionization techniques in either the upper or lower level, as is well known from the *one-atom-maser* operation [13–15].

There have been theoretical studies on reconstructing the micromaser state by probing it with two-level atoms [9]. In these investigations, the atoms have to be prepared in a *coherent superposition* between the upper and lower levels. In the present suggestion, however, we restrict ourselves to the initial atomic preparation in an energy eigenstate, and are moreover completely independent of the information about the superposition *phase* at any time. For this reason, we do not have to worry about the destruction of the coherence of the atomic superposition that can easily occur in the presence of weak electric stray fields, for example, in the cavity entrance holes.

For the investigation of quantized atomic motion the Jaynes-Cummings model has been introduced, and several schemes have been proposed for the reconstruction of quantum-mechanical vibrational states of a trapped atom [10]. Leibfried *et al.* showed experimentally that the vibrational mode can be reconstructed in the number state basis as well as in terms of the Wigner function [11]. In their experiment, an initial state is coherently displaced along a circle in phase space, and the statistics of the atomic inversion are measured for various interaction times. The time-dependent statistics are converted into the phonon number distribution of the displaced states. Using the relation between the phonon number statistics of the displaced state and the density matrix [7,8] or the Wigner function [16], respectively, they found the original motional quantum state in these two representations. In this paper, we use a related approach in order to probe the micromaser field. However, instead of collecting the atomic statistics for various interaction times, we leave this parameter fixed. This method is more robust against cavity decay, and experimentally more feasible for probing the micromaser field. Moreover, we avoid the method via the

*On leave from Department of Physics, Sogang University, C.P.O. Box 1142, Seoul, Korea.

displaced photon number distribution for the reconstruction of the density matrix and perform a rather straightforward method, which makes the numerical calculation more stable.

II. ATOMIC EMISSION PROBABILITY FOR DISPLACED FIELD STATES

The experimentally observable system is *not* the state of the cavity field itself but rather the atoms after their interaction with the field. In this section we will investigate the atomic inversion in combination with a displacement of the initial field state.

We start with the single-mode radiation field inside a cavity initially prepared in a state represented by a density matrix ρ , which shall be reconstructed. Possible preparation techniques are discussed below. Now we perform a displacement of the initial state in phase space by applying a unitary transformation $D(\alpha)\rho D^\dagger(\alpha)$, with the displacement operator

$$D(\alpha) = \exp(\alpha a^\dagger - \alpha^* a). \quad (1)$$

Here a and a^\dagger are the annihilation and creation operators, and α is a complex number characterizing the amplitude and phase of the shift. Experimentally this operation is carried out by coupling a resonant classical oscillator to the cavity field. The time evolution (in an interaction picture rotating with the cavity frequency) of the driven cavity field is then determined by the Hamiltonian $H_{\text{osc}} = \hbar(fa^\dagger + f^*a)$ [17], with f being a scaled classical field amplitude. Replacing α by $-ift$ in Eq. (1) leads immediately to the unitary time evolution of the driven cavity. However, the duration required for the shift has to be chosen small compared to the cavity damping time t_{cav} , a condition that can always be fulfilled, if only $|f|$ is chosen large enough.

Now we inject an atom prepared in one of its two considered energy levels, e.g., the upper one $|e\rangle$. (Atoms usually begin from an opening in a thermal oven, and therefore have random Poisson distributed arrival times. So the atomic flux must be large enough to keep the average temporal spacing of the atoms small compared to t_{cav} . If the waiting time for the next atom should still be unexpectedly long, we can just disregard these single events.) During the atom-field interaction time τ , dissipation can again be disregarded in a very good approximation, because of τ typically being *much* smaller than t_{cav} . This leads to a Jaynes-Cummings-type interaction [12] resulting in a new density matrix

$$\mathcal{S}(\alpha, \tau) = U^\dagger(\tau)[D(\alpha)\rho D^\dagger(\alpha) \otimes |e\rangle\langle e|]U(\tau), \quad (2)$$

with the unitary time evolution operator $U(\tau)$. In this *entangled* atom-field state, we ask for the probability p_g to find the atom in the lower state $|g\rangle$, or, in other words, for the expectation value of the projection operator $|g\rangle\langle g|$ (operators of one of the two subspaces *alone* are looked upon as extended by the unity operator of the other subspace):

$$\begin{aligned} p_g(\alpha, \tau) &= \text{Tr}\{\mathcal{S}(\alpha, \tau)|g\rangle\langle g|\} \\ &= \text{tr}_f\{D(\alpha)\rho D^\dagger(\alpha)\langle e|U(\tau)|g\rangle\langle g|U^\dagger(\tau)|e\rangle\}. \end{aligned} \quad (3)$$

Tr denotes the complete trace, whereas tr_f relates only to the field. For the sake of simplification, we assume exact resonance between atoms and the cavity field, and rewrite the Jaynes-Cummings time evolution operator [12] $U(\tau) = \exp\{-i\lambda\tau(\sigma a^\dagger + \sigma^\dagger a)\}$ (σ and σ^\dagger are the atomic ‘‘spin-flip’’ operators, and λ stands for the dipole coupling strength) in the following way [18]:

$$\begin{aligned} U(\tau) &= \cos(\lambda\tau\sqrt{\hat{n}+1})|e\rangle\langle e| + \cos(\lambda\tau\sqrt{\hat{n}})|g\rangle\langle g| \\ &\quad - i\frac{\sin(\lambda\tau\sqrt{\hat{n}+1})}{\sqrt{\hat{n}+1}}a|e\rangle\langle g| - i\frac{\sin(\lambda\tau\sqrt{\hat{n}})}{\sqrt{\hat{n}}}a^\dagger|g\rangle\langle e|, \end{aligned} \quad (4)$$

with the photon number operator $\hat{n} = a^\dagger a$. Substituting this expression into Eq. (3), we arrive at

$$p_g(\alpha, \tau) = \text{tr}_f\{\rho D^\dagger(\alpha)\sin^2(\sqrt{\hat{n}+1}\lambda\tau)D(\alpha)\}. \quad (5)$$

This is obviously the expectation value of the operator $D^\dagger(\alpha)\sin^2(\sqrt{\hat{n}+1}\lambda\tau)D(\alpha)$ expressed in terms of the *initial* field state ρ . Without the application of the displacement operator $D(\alpha)$ this observable would merely be a function of \hat{n} , and therefore supply *no phase information*. Only the combination with the displacement leads to a *phase-sensitive* observable.

For further calculations, the trace is performed in the Fock base:

$$p_g(\alpha, \tau) = \sum_{n=0}^{\infty} \langle n|D(\alpha)\rho D^\dagger(\alpha)|n\rangle \sin^2(\sqrt{n+1}\lambda\tau). \quad (6)$$

We recognize the photon number distribution of the shifted field state or, from another point of view, the overlap of shifted Fock states with the initial field state entering this formula. We will in contrast to other calculations [11], not solve Eq. (6) for these numbers. For analyzing Eq. (6), we express the operators ρ and $D(\alpha)$ in number states

$$\rho = \sum_{n=0}^{\infty} \rho_n^{(0)}|n\rangle\langle n| + \left\{ \sum_{k=1}^{\infty} \sum_{n=0}^{\infty} \rho_n^{(k)}|n\rangle\langle n+k| + \text{H.c.} \right\}, \quad (7)$$

$$D(\alpha) = \sum_{n,m=0}^{\infty} d_{nm}(\alpha)|n\rangle\langle m|, \quad (8)$$

where H.c. stands for the Hermitian conjugate. The matrix elements d_{nm} of the displacement operator (depending on $\alpha = r e^{i\phi}$ expressed in polar coordinates with real parameters r and ϕ) are given by [19,20]

$$\begin{aligned} d_{nm}(\alpha) &= \begin{cases} \sqrt{\frac{m!}{n!}} e^{-1/2r^2} r^{n-m} e^{i(n-m)\phi} \mathcal{L}_m^{n-m}(r^2) & \text{for } n \geq m \\ d_{mn}^*(-\alpha) & \text{for } n \leq m, \end{cases} \end{aligned} \quad (9)$$

with the associated Laguerre polynomials, $\mathcal{L}_m^n(x)$. Substituting Eqs. (7) and (8) into Eq. (6) yields the following expression for the atomic emission probability:

$$p_g(r, \phi) = \sum_{n,m=0}^{\infty} \sin^2(\sqrt{m+1}\lambda\tau) \mathcal{X}_{mn}^{(0)}(r) \rho_n^{(0)} + 2 \operatorname{Re} \sum_{k=1}^{\infty} \sum_{n,m=0}^{\infty} \sin^2(\sqrt{m+1}\lambda\tau) \times \mathcal{X}_{mn}^{(k)}(r) \rho_n^{(k)} e^{ik\phi}. \quad (10)$$

In this paper the interaction time is assumed to be fixed, so the argument τ has been dropped to simplify the notation. Moreover, we introduced the definition

$$\mathcal{X}_{mn}^{(k)}(r) e^{ik\phi} = d_{mn}(\alpha) d_{(n+k)m}(-\alpha), \quad (11)$$

where $\mathcal{X}_{mn}^{(k)}(r)$ turns out to be a *real* number.

Equation (10) shows that the observable p_g depends in principle on *all* matrix elements of the initial field state ρ . From a mathematical point of view, one could simply determine a sufficient number of atomic emission probabilities for different displacements, and solve the emerging system of linear equations for the unknowns $\rho_n^{(k)}$ in a reasonably truncated Fock space. However, this method has little practical use because these systems of equations are frequently close to singularity and very sensible to noisy data. That is why it will be a task of Sec. III to find equations which separate the matrix elements for each diagonal specified by the integer k .

III. RECONSTRUCTION AND ANALYSIS

We realize Eq. (10) to be a Fourier sum for p_g looked upon as a 2π -periodic function in ϕ with fixed amplitude r . Turning to the Fourier amplitudes of the oscillations $e^{ik\phi}$, defined by

$$q^{(k')}(r) = \frac{1}{2\pi} \int_0^{2\pi} p_g(r, \phi) e^{-ik'\phi} d\phi \quad (12)$$

($k' = 0, 1, \dots$), yields, with the help of the Fourier representation of the Kronecker δ symbol

$$\delta_{k,k'} = \frac{1}{2\pi} \int_0^{2\pi} e^{i(k-k')\phi} d\phi, \quad (13)$$

the following expression (we replace k' by k):

$$q^{(k)}(r) = \sum_{n,m=0}^{\infty} \sin^2(\sqrt{m+1}\lambda\tau) \mathcal{X}_{mn}^{(k)}(r) \rho_n^{(k)} = \sum_{n=0}^{\infty} \mathcal{Y}_n^{(k)}(r) \rho_n^{(k)}. \quad (14)$$

The sum over m has been summarized as $\sum_{m=0}^{\infty} \sin^2(\sqrt{m+1}\lambda\tau) \mathcal{X}_{mn}^{(k)}(r) = \mathcal{Y}_n^{(k)}(r)$.

We recognize that the discrete spectrum of the atomic emission probability, regarded as a function of ϕ on a circle

with radius r in phase space, separates the single diagonals of ρ . The amplitude of the k th harmonic oscillation depends *only* on the k th diagonal [21].

Integrals like Eq. (12), already requiring in principle an infinite number of probabilities, are mathematical rather than physical constructions. In reality we will have to restrict ourselves to a finite number L of angles $\phi_l = (2\pi/L)l$ with $l \in \{0, 1, \dots, L-1\}$, and replace Eq. (12) by a *discrete* Fourier transform labeled with the additional parameter L :

$$q_L^{(k')}(r) = \frac{1}{L} \sum_{l=0}^{L-1} p_g(r, \phi_l) e^{-ik'\phi_l}. \quad (15)$$

Applying this transform to Eq. (10) no longer yields Eq. (13), but rather

$$\frac{1}{L} \sum_{l=0}^{L-1} e^{i(k-k')\phi_l}. \quad (16)$$

This expression still behaves like the Kronecker δ symbol, at least if $k-k'$ is not an integer multiple of L . However, for $k-k' = \pm sL$ with $s=1, 2, \dots$, we obtain an additional ‘‘1’’ instead of a ‘‘zero.’’ For this reason, the approximated Fourier transform Eq. (15) leads to Eq. (14) *plus* some residual terms:

$$q_L^{(k)}(r) = q^{(k)}(r) + \sum_{n,m=0}^{\infty} \sin^2(\sqrt{m+1}\lambda\tau) \times \left\{ \sum_{s=1}^{\infty} \mathcal{X}_{mn}^{(qL+k)} \rho_n^{(qL+k)} + \sum_{sL-k>0} \mathcal{X}_{mn}^{(sL-k)} \times (\rho_n^{(sL-k)})^* + \sum_{-sL+k>0} \mathcal{X}_{mn}^{(-sL+k)} \rho_n^{(-sL+k)} \right\}. \quad (17)$$

Let us illuminate this expression in combination with a truncated Fock space, and assume that $\rho_n^{(k)} \approx 0$ for $n+k > N$. N is the highest photon number still taken into account. It is inevitable to add some *a priori* information for a reasonable choice of it. If we demand the condition $L-k \geq N+1$, then all matrix elements of ρ in the additional terms of Eq. (17) are already beyond the restricted Fock space, and therefore considered to be zero. This holds for all Fourier amplitudes in the truncated Fock space if we set $k=N$. Therefore the adapted number of angles L for the $(N+1)$ -dimensional Fock space is

$$L \geq 2N+1. \quad (18)$$

If the field state is really (not just approximately) limited to N photons, then a phase discretization fulfilling Eq. (18) does not lead to any error at all. This is in agreement with the result derived by Opatný *et al.* [8] for the unbalanced homodyne measurement.

Now we turn back to Eq. (14), rewritten for a $(N+1)$ -dimensional Fock space with L discrete angles:

$$q_L^{(k)}(r_j) = \sum_{n=0}^{N-k} \mathcal{Y}_n^{(k)}(r_j) \rho_n^{(k)}. \quad (19)$$

For any practical calculation, the m sum in Eq. (14) will also be truncated at a maximum photon number M adapted to the *displaced* field state. [M can be estimated as $M=(c r_j + \sqrt{N+1})^2$ with a constant number c in the order of 3.]

Equation (19) represents a system of linear equations for the $N+1-k$ unknown $\rho_n^{(k)}$'s of the k th diagonal of the density matrix. For an unambiguous solution, at least the same number of independent equations is required. Therefore we choose $j=1, \dots, N+1-k$ (or more) different radii r_j . [We recall that the Fourier amplitudes $q_L^{(k)}(r, \tau)$ still depend on the interaction time τ . So it would in principle also be possible to restrict oneself to one single radius and choose $N+1-k$ different times τ_i . We believe, however, that from the experimental point of view it is more convenient to fix one single interaction time for the whole reconstruction, because a variation of τ in a large regime results in a rather small atomic flux for the extreme interaction times due to the (modified) thermal velocity distribution [22] of the atomic beam.] For each radius, measurements for at least $N+1+k$ angles are necessary (see above). Thus the determination of all matrix elements of a k th diagonal requires the measurement of $(N+1-k)(N+1+k)=(N+1)^2-k^2$ emission probabilities. However, for the complete reconstruction (in the restricted Fock space) $2N+1$ angles [Eq. (18)] on $N+1$ radii, and thus

$$(N+1)^2 + N^2 + N \quad (20)$$

measured probabilities are necessary. On the other hand, there are $(N+1)^2$ unknowns whereby the complex off-diagonals are counted twice.

IV. ERROR ESTIMATION AND NUMERICAL METHODS

We now turn to the problem of how to solve Eq. (19) for the matrix elements $\rho_n^{(k)}$. For convenience we shall first rewrite it in the familiar matrix notation

$$\vec{q}^{(k)} = \mathbf{Y}^{(k)} \vec{\rho}^{(k)}. \quad (21)$$

The coefficients $\mathbf{Y}_{jn}^{(k)}$ of the $J \times (N+1-k)$ matrix $\mathbf{Y}^{(k)}$ (with $J \geq N+1$ different radii r_j) are related to Eq. (19) via $\mathbf{Y}_{jn}^{(k)} \equiv \mathcal{Y}_n^{(k)}(r_j)$. The vectors $\vec{\rho}^{(k)}$ and $\vec{q}^{(k)}$ contain the unknowns $\rho_n^{(k)}$ and the Fourier amplitudes $q_j^{(k)} \equiv q_L^{(k)}(r_j)$, respectively. To simplify the notation we drop the index (k) .

The solution of Eq. (21) is not unique as soon as there exist nontrivial solutions to the homogeneous equation $\mathbf{Y} \vec{\rho} = \vec{0}$. However, the vector $\vec{\rho}_{\min}$ with the smallest norm $|\vec{\rho}_{\min}|$ among all possible solutions is unique. The *pseudoinverse* $\bar{\mathbf{Y}}$ of the matrix \mathbf{Y} is defined via the equation [23,24]

$$\vec{\rho}_{\min} = \bar{\mathbf{Y}} \vec{q}. \quad (22)$$

Now we wish to take into consideration that the experimentally determined data are never exact but rather subject to various measurement errors. Most of these errors appear via the measured probabilities p_g in the Fourier amplitudes q_L in Eq. (15). For this reason it is of particular interest to examine the error $\Delta \vec{\rho}_{\min}$ due to a perturbation $\Delta \vec{q}$ in the modified equation $\vec{q} + \Delta \vec{q} = \mathbf{Y}(\vec{\rho} + \Delta \vec{\rho})$. This yields

$$\Delta \vec{\rho}_{\min} = \bar{\mathbf{Y}} \Delta \vec{q}. \quad (23)$$

For further diagnosis and error estimation, the method of *singular value decomposition* [23,24] provides a powerful set of tools. It is based on the possibility of decomposing any arbitrary matrix \mathbf{Y} into a product of three matrices in the form

$$\mathbf{Y} = \mathbf{U} \mathbf{W} \mathbf{V}^T. \quad (24)$$

\mathbf{U} is in our case a $J \times (N+1-k)$ column-orthogonal, \mathbf{W} an $(N+1-k) \times (N+1-k)$ diagonal, and \mathbf{V} an $(N+1-k) \times (N+1-k)$ orthogonal matrix. The uniquely determined diagonal elements $\mathbf{W}_{nn} \equiv w_n$ (*singular values*) are the positive square roots of the eigenvalues of the matrix $\mathbf{Y}^T \mathbf{Y}$. The pseudo inverse $\bar{\mathbf{Y}}$ can explicitly be expressed as $\bar{\mathbf{Y}} = \mathbf{V} \bar{\mathbf{W}} \mathbf{U}^T$ with the matrix elements $\bar{\mathbf{W}}_{nm} = (1/w_n) \delta_{nm}$ if $w_n \neq 0$. If vanishing singular values occur, the respective $\bar{\mathbf{W}}_{nn}$ are equated to zero.

By means of the smallest not vanishing and the largest singular value w_{\min} and w_{\max} the absolute and relative error can be estimated as [24]

$$|\Delta \vec{\rho}_{\min}| \leq \frac{1}{w_{\min}} |\Delta \vec{q}| \quad (25)$$

and

$$\frac{|\Delta \vec{\rho}_{\min}|}{|\vec{\rho}_{\min}|} \leq \frac{w_{\max}}{w_{\min}} \frac{|\Delta \vec{q}|}{|\mathbf{P}_{\text{map}(Y)} \vec{q}|}. \quad (26)$$

Here $\mathbf{P}_{\text{map}(Y)}$ denotes the projection into the range of \mathbf{Y} . Equation (26) is governed by the ratio w_{\max}/w_{\min} which is a possible (not unique but up to our experience especially useful) definition of the *condition number*.

A frequently appearing problem is that of ‘‘ill-conditioned’’ matrices: Tiny perturbations are intensified by an extremely high condition number and lead to huge errors. In this case $\bar{\mathbf{Y}}$ can be replaced by a *regularized* matrix $\bar{\mathbf{Y}}^{\text{reg}}$ that arises from $\bar{\mathbf{Y}}$ by zeroing all diagonal elements of $\bar{\mathbf{W}}$ that go beyond a certain parameter of regularization. This way we arrive at a solution $\vec{\rho}_{\min}^{\text{reg}} = \bar{\mathbf{Y}}^{\text{reg}} \vec{q}$ for an approximation $\vec{q} = \mathbf{Y}^{\text{reg}} \vec{\rho}^{\text{reg}}$ of Eq. (21), with an improved condition. Thus the sensitivity to perturbations decreases as expressed in Eqs. (25) and (26). But there is a price to pay: A systematic error is added, which is *not* covered by these equations. In the regularized problem the number of free parameters (which is equal to the number of nonzero $\bar{\mathbf{W}}_{nn}$'s) is reduced. This leads to a tendency of the solution vector to become smaller in magnitude but much more stable to perturbations. In our experience, in a ‘‘well-regularized’’ problem the dependence of the solution on the exact number of removed singularities is only weak. The systematic error can be estimated by simply substituting the vector $\vec{\rho}_{\min}^{\text{reg}}$ back into the initial Eq. (21).

In Sec. V we will deal with an overdetermined system ($J > N+1$) in combination with noisy data. In this case we do not expect that there is an exact solution of Eq. (21) at all,

because noisy data is contradictory. Thus we look for the best approximation in the sense of minimizing the expression [25]

$$\chi^2 = |\vec{q} - \mathbf{Y} \vec{\rho}|^2. \quad (27)$$

Singular value decomposition already provides the right answer; it is still given by Eq. (22). In combination with regularization, χ^2 increases for each singular value that is zeroed because of the additional systematic error. (If this is not the case, then the rounding error in the numerical calculation becomes relevant.) Due to the reduction of free parameters the noisy data are no longer fitted in too many details but rather smoothly. This is exactly what we want.

We will now briefly discuss possible errors arising from nonideal experimental conditions. The statistical error due to a finite number of measurements is especially fundamental. Let Z be the number of measurements for the determination of each probability p_g . Then the standard deviation Δp_g is given by $\Delta p_g = \sqrt{p_g(1-p_g)/Z} \leq 1/(2\sqrt{Z})$. Thus the Fourier amplitudes $q_L^{(k)}$ are affected with a standard deviation $\Delta q_L^{(k)} = (1/\sqrt{L})\Delta p_g \leq 1/(2\sqrt{LZ})$. In Sec. V the effect of this statistical error will be calculated for the example of a simulated reconstruction.

The interaction time τ is also a very important parameter. The method of oblique excitation takes advantage of the Doppler effect and combines a high atomic flux with a very good velocity selection. A typical value for $\Delta\tau/\tau$ is 2%. If necessary, the control of this parameter can be even improved by decreasing the angle between atoms and laser beam which will however reduce the atomic flux.

Errors could also occur due to mechanical vibrations of the cavity. This would lead to a detuning and thus to an inaccuracy in the displacement.

Systematic errors appear because of the finite detector efficiencies (typically less than $\frac{1}{2}$), the truncation of the Fock space and the discretization of angles in the Fourier transform Eq. (15), as calculated in Eq. (17). The best way to find a reasonable ‘‘cutoff photon number’’ N is probably just to try a few different choices. If N is sufficiently large, the result of the reconstruction is almost independent of it. If it becomes too large, the error increases. This is how we deal with this problem in the simulation (Sec. V).

Spontaneous decays of the atoms into deeper-lying states are another source of inaccuracy. However, the lifetime of high-lying Rydberg states is quite large compared to the relevant time constants of the experiment.

V. COMPUTER SIMULATION

We would like to show the usefulness of our reconstruction scheme by performing a computer simulation in consideration of measurement errors. Therefore we first turn back to the problem of preparing the initial field state.

It is likely to start with the so-called ‘‘stationary micromaser state,’’ that builds up after a successive interaction of many inverted two-level atoms with the cavity field [13–15]. This state shows several nonclassical features, the best known of which is probably the sub-Poissonian photon number distribution appearing in a wide regime of operation. All off-diagonal elements $\rho_n^{(k)}$ for $k > 0$ are equal to zero, which

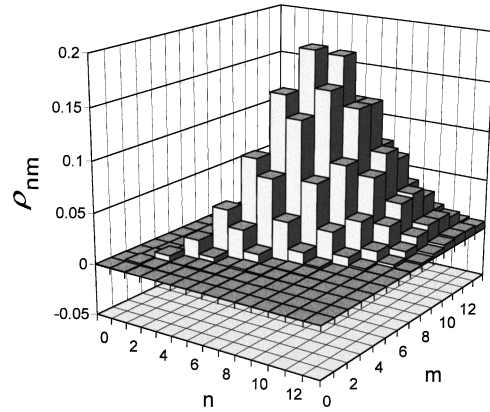


FIG. 1. Density-matrix elements $\rho_{nm} \equiv \rho_n^{(k=m-n)}$ of the seeded micromaser field in the Fock representation. The field is generated in the micromaser cavity by simultaneous atomic pumping and coupling to a classical oscillator. This way, a sub-Poissonian photon number distribution is combined with a well-defined field phase. The parameters are $N_{\text{ex}}=10$, $\theta=3$, $\langle n_{\text{osc}} \rangle = 4|f|^2 t_{\text{cav}}^2 = 6.25$, $T = 500$ mK, $\langle n \rangle = 7.4$, and $Q = -0.42$.

means that no preferred field phase exists. In other words, the phase-space distributions (e.g., P , Q , or Wigner function) are radially symmetric. The emission probability $p_g(r, \phi)$ in Eq. (10) becomes consequently independent of the angle ϕ , and we further find $q_L^{(0)}(r) = p_g(r)$ and $q_L^{(k)}(r) = 0$ for $k > 0$ [Eq. (15)]. Therefore Eq. (19) as well as Eq. (10) simply reduce to

$$p_g(r_j) = \sum_{n=0}^N \mathcal{J}_n^{(0)}(r_j) \rho_n^{(0)}. \quad (28)$$

Thus we arrive at a nice method for the reconstruction of the photon number distribution: We just need to measure $N+1$ (or more) probabilities p_g at different radii r_j , and solve for the values $\rho_n^{(0)}$. Measurements on the photon statistics inside a high- Q cavity were performed by Brune *et al.* [26]. Instead of shifting the field state, they observed the atomic Rabi oscillations on the dependence on the interaction time.

The reconstruction scheme unfolds its usefulness completely for field states without the radial symmetry. A phase-dependent state could simply be built up by coupling the cavity to a weak classical oscillator which will afterwards perform the displacement. This yields the preparation of a ‘‘shifted’’ thermal state which approaches for the cavity temperature $T \rightarrow 0$ asymptotically to the well-known coherent state.

A more interesting situation arises if both, the atomic pumping and a weak coupling to the classical oscillator, are combined. Therefore, we first prepare the cavity field in a stationary micromaser state characterized by the ‘‘effective pumping rate’’ $N_{\text{ex}} = r t_{\text{cav}} = 10$ (r is the atomic rate) and the ‘‘pumping parameter’’ $\Theta = \sqrt{N_{\text{ex}}} \lambda \tau = 3$. This state has a mean photon number $\langle n \rangle = 5.2$. For a quantitative measure of the non-Poissonian characteristic of the photon number distribution, the normalized variance $Q = (\langle n^2 \rangle - \langle n \rangle^2) / \langle n \rangle - 1$ is frequently used. For a state with Poissonian photon statistics, we find $Q = 0$ whereas a sub-Poissonian state is characterized by negative- Q values. The micromaser state in our example yields $Q = -0.56$. Now we *additionally* drive the

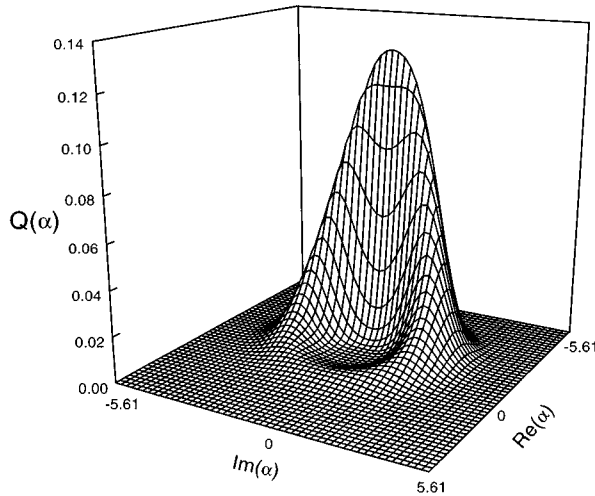


FIG. 2. Same state as in Fig. 2 in Q representation.

field with the classical oscillator. The irreversible time evolution of the field state is therefore governed by the following linear quantum master equation

$$\frac{\partial}{\partial t} \rho = (r\mathcal{M}_0 + \mathcal{L})\rho - \frac{i}{\hbar} [H_{\text{osc}}, \rho]. \quad (29)$$

\mathcal{M}_0 denotes the operator describing the pumping effect of the atoms arriving at random with rate r , while \mathcal{L} stands for the Liouville operator that estimates the decay toward the thermal state. The explicit expressions for these operators are found in Ref. [27] (we use the same nomenclature as there). The additional commutator, with the Hamiltonian H_{osc} introduced in Sec. II, describes the effect of the coupling between cavity field and classical oscillator.

We numerically integrate Eq. (29) to find the new stationary solution, which we call the *seeded micromaser state*. The outgoing density matrix in the Fock representation is presented in Fig. 1. We recognize off-diagonal elements arising; they indicate that coherences between number states build up. To gain more graphic insight into the characteristics of a

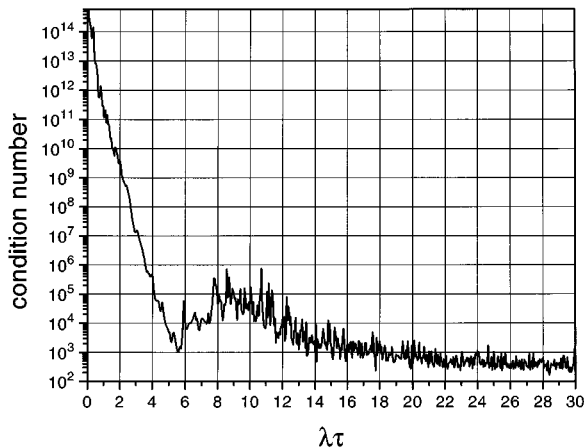


FIG. 3. Dependence of the condition number $w_{\text{max}}/w_{\text{min}}$ on the scaled interaction time $\lambda\tau$ for the example of the main diagonal of the density matrix. Large interaction times improve the condition dramatically.

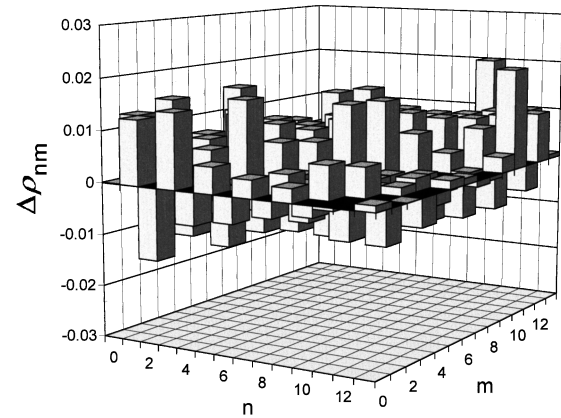


FIG. 4. Estimation of the statistical error according to Eq. (23) for the regularized problem. The perturbation $\Delta\vec{q}$ equals the standard deviation due to a number of 2500 measurements for the determination of each probability p_g . The condition number is in the order of 100 for the main diagonal and less for the off-diagonal elements.

quantum state, quasiprobability distributions in phase space such as the Q , Wigner, or P function [19] are useful. The Q function, simply defined as $Q(\alpha) = \langle \alpha | \rho | \alpha \rangle / \pi$, is shown in Fig. 2 for the seeded micromaser state. The field takes the phase of the classical oscillator, while the sub-Poissonian characteristics of the stationary micromaser state is hardly affected [28]. We now find $\langle n \rangle = 7.4$ and $Q = -0.42$.

For the reconstruction, we took advantage of the *mirror symmetry* in phase space with respect to an axis, which can (without restriction of generality) be defined as the real one $[\text{Re}(\alpha)]$. In this case it can easily be shown that all matrix elements $\rho_n^{(k)}$ are *real* numbers, and thus the number of unknowns reduces to $(N+1)(N+2)/2$. Moreover, a mirror symmetric state displaced by an amount α is identical to the one arising from a displacement characterized by α^* , except their phases, which do *not* affect the atomic emission probability (see above). This yields $p_g(\alpha) = p_g(\alpha^*)$, and causes

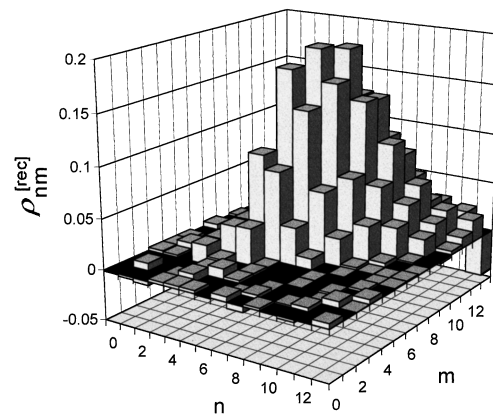


FIG. 5. Result of a reconstruction of the field state depicted in Fig. 1. Measurement errors are considered by adding a Gauß-distributed noise to the calculated probabilities p_g with a standard deviation of 0.01. Displacements are performed to 16 locations along 30 semicircles with radii that increase by a step of 0.4. The scaled interaction time $\lambda\tau$ is 3.16, and the Fock space is restricted to $N=13$ photons.

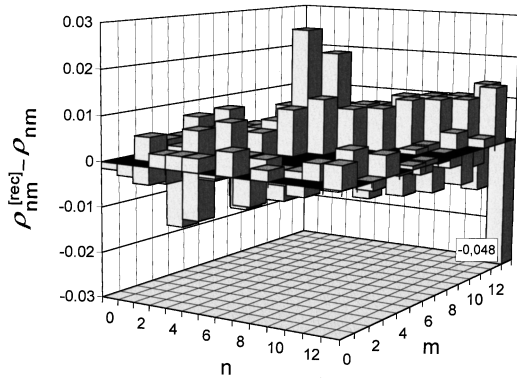


FIG. 6. Deviation between exact and reconstructed values of the density matrix.

the Fourier components [Eq. (15)] to become *real* numbers. Thus it is sufficient to restrict the displacements to locations along *semicircles* in phase space with only positive (or only negative) imaginary parts of α . Consequently the minimum number of probabilities p_g to be measured [Eq. (20)] reduces to $(N+1)^2$ and $(N+1)^2 + (N+1)/2$ for *odd* and *even* numbers L of discrete angles, respectively. (In the first case we have only one displacement with *real* α , whereas in the second case there are two such events, which causes the difference.)

Now we simulate displacements to 16 locations each along 30 semicircles with radii that increase by steps of 0.4. The Fock space is restricted to $N=13$ photons (see Sec. IV for an estimation of the number N). Before we carry out the reconstruction, we consider the condition (Sec. IV) of this problem. Figure 3 shows that there is a very strong dependence of the condition number on the scaled interaction time $\lambda\tau$. It decreases approximately exponentially with increasing $\lambda\tau$ up to a value of $\lambda\tau \approx 5.5$. In our simulation we make a compromise between good condition and experimentally well feasible parameters, and choose $\lambda\tau = 3.16$. Most of the possible errors discussed in Sec. IV are strongly dependent on the details of an experimental realization, and are currently hard to estimate. We will therefore restrict ourselves to the statistical error, which is a general property. We choose a number of $Z=2500$ measurements for the determination of each probability p_g , and obtain a Gauß-distributed noise with a standard deviation of 0.01 which is added to the calculated values. Equation (26) signifies that the condition number should not exceed the order of 100 too much in order to obtain reasonable results. A detailed estimation of the statistical error for the individual matrix elements is given in Fig. 4. It shows $\Delta \vec{\rho}_{\min}$ according to Eq. (23) for the regularized problem. The perturbation is estimated by setting all components of $\Delta \vec{q}$ equal to the standard deviation $\Delta q_L^{(k)}$ (see Sec. IV).

The reconstructed density matrix is plotted in Fig. 5. Figure 6 shows the deviation between exact and reconstructed values of the matrix elements. We find a satisfactory agree-

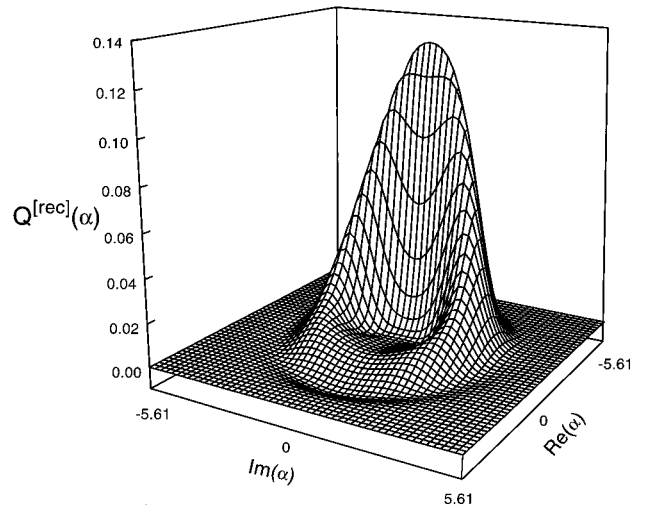


FIG. 7. Q representation for the reconstructed field. (Parameters as in Fig. 5).

ment between them. This is also confirmed by the Q representation of the quantum state calculated from the reconstructed density matrix, as shown in Fig. 7. However, some slight negative values occur in the reconstructed Q function even though the Q function of a physical state is certainly always positive.

VI. CONCLUSION

In this paper we showed how to reconstruct the quantum state of a single-mode microwave field inside a high- Q cavity with the method of coherent displacements in phase space, and subsequent probing by two-level atoms. We intentionally did not use atomic coherences or the variation of additional parameters such as the interaction time to keep the method as easily feasible as possible. The displacements are performed to several points along circles of different radii. We pointed out a relation between the spectrum of the atomic emission probability and the single diagonals of the field density matrix. This relation yields a system of linear equations for each diagonal, that can easily be inverted to find the matrix elements. The reconstruction scheme was demonstrated with the example of a seeded micromaser state.

Finally we would like to remark that the decay of the Fourier component $q^{(1)}(r,t)$, in Eq. (14), is well suited for the observation of the phase diffusion. The time dependence of Eq. (14) is strongly related to that of the expectation value of the electric-field strength, and therefore to the *micromaser spectrum* [29].

ACKNOWLEDGMENTS

G.A. and C.T.B. thank G. Raithel and S. Wallentowitz for inspiring discussions, and A. Prinz for reading the manuscript. M.S.K. thanks the Alexander von Humboldt Foundation for support.

- [1] K. Vogel and H. Risken, *Phys. Rev. A* **40**, 2847 (1989).
- [2] V. Bužek, G. Adam, and G. Drobný, *Phys. Rev. A* **54**, 804 (1996).
- [3] N. G. Walker and C. A. Carroll, *Opt. Quantum Electron.* **18**, 355 (1986); J. W. Noh, A. Fougères, and L. Mandel, *Phys. Rev. Lett.* **71**, 2579 (1993); D. T. Smithey, M. Beck, M. Belsley, and M. G. Raymer, *ibid.* **69**, 2650 (1992).
- [4] S. Schiller, G. Breitenbach, S. F. Pereira, T. Müller, and J. Mlynek, *Phys. Rev. Lett.* **77**, 2933 (1996).
- [5] S. Wallentowitz and W. Vogel, *Phys. Rev. A* **53**, 4528 (1996).
- [6] K. Banaszek and K. Wódkiewicz, *Phys. Rev. Lett.* **76**, 4344 (1986).
- [7] T. Opatrny and D.-G. Welsch, *Phys. Rev. A* **55**, 1462 (1997).
- [8] T. Opatrny, D.-G. Welsch, S. Wallentowitz, and W. Vogel, *J. Mod. Opt.* (to be published).
- [9] P. J. Bardroff, E. Mayr, and W. P. Schleich, *Phys. Rev. A* **51**, 4963 (1995); L. G. Lutterbach and L. Davidovich, *Phys. Rev. Lett.* **78**, 2547 (1997).
- [10] S. Wallentowitz and W. Vogel, *Phys. Rev. Lett.* **75**, 2932 (1995); J. F. Poyatos, R. Walser, J. I. Cirac, P. Zoller, and R. Blatt, *Phys. Rev. A* **53**, 1966 (1996); C. D'Helon and G. J. Milburn, *ibid.* **54**, 25 (1986); P. J. Bardroff, C. Leichtle, G. Schrade, and W. P. Schleich, *Phys. Rev. Lett.* **77**, 2198 (1996); M. Freyberger, *Phys. Rev. A* **55**, 4120 (1997).
- [11] D. Leibfried, D. M. Meekhof, B. E. King, C. Monroe, W. M. Itano, and D. J. Wineland, *Phys. Rev. Lett.* **77**, 4281 (1996).
- [12] B. W. Shore and P. L. Knight, *J. Mod. Opt.* **40**, 1195 (1993).
- [13] P. Filipowicz, J. Javanainen, and P. Meystre, *Phys. Rev. A* **34**, 3077 (1986); L. A. Lugiato, M. O. Scully, and H. Walther, *ibid.* **36**, 740 (1987).
- [14] D. Meschede, H. Walther, and G. Müller, *Phys. Rev. Lett.* **54**, 551 (1985); G. Rempe, H. Walther, and N. Klein, *ibid.* **58**, 353 (1987); G. Rempe, F. Schmidt-Kaler, and H. Walther, *ibid.* **64**, 2783 (1990).
- [15] Recent reviews are given in G. Raithel, Ch. Wagner, H. Walther, L. M. Narducci, and M. O. Scully, in *Advances in Atomic, Molecular and Optical Physics*, edited by P. Berman (Academic, New York, 1994), Suppl. 2; H. Walther, in *Quantum Optics and the Spectroscopy of Solids*, edited by T. Hakioğlu and A. S. Shumovsky (Kluwer, Dordrecht, 1997).
- [16] H. Moya-Cessa and P. L. Knight, *Phys. Rev. A* **48**, 2479 (1993).
- [17] See for example, W. H. Louisell, *Quantum Statistical Properties of Radiation* (Wiley, New York, 1973).
- [18] S. Stenholm, *Phys. Rep.* **6C**, 1 (1973).
- [19] K. E. Cahill and R. J. Glauber, *Phys. Rev.* **177**, 1857 (1969).
- [20] F. A. M. de Oliveira, M. S. Kim, P. L. Knight, and V. Bužek, *Phys. Rev. A* **41**, 2645 (1990).
- [21] It is remarkable that the same dependence is observed in the Fourier-spectrum of quasiprobability distributions as Q , Wigner, or P functions.
- [22] N. F. Ramsey, *Molecular Beams* (Oxford University Press, Oxford, 1956).
- [23] G. H. Golub and C. F. van Loan, *Matrix Computations* (Johns Hopkins University Press, Baltimore, 1989); W. H. Press, S. A. Teukolsky, W. T. Vetterling, and B. P. Flannery, *Numerical Recipes in C* (Cambridge University Press, Cambridge, 1995).
- [24] G. Hämmerlin and K. H. Hoffman, *Numerische Mathematik* (Springer-Verlag, Berlin, 1991).
- [25] Least χ^2 fitting is the adequate method, if the errors are independent and normally distributed with constant standard deviation or close to these conditions.
- [26] M. Brune, F. Schmidt-Kaler, A. Maali, J. Dreyer, E. Hagley, J. M. Raimond, and S. Haroche, *Phys. Rev. Lett.* **76**, 1800 (1996).
- [27] H.-J. Briegel, B.-G. Englert, N. Sterpi, and H. Walther, *Phys. Rev. A* **49**, 2962 (1994).
- [28] The contour lines of the Q function remind one very much of the shape of a banana; this is why we sometimes speak about the "banana state."
- [29] T. Quang, G. S. Agarwal, J. Bergou, M. O. Scully, H. Walther, K. Vogel, and W. P. Schleich, *Phys. Rev. A* **48**, 803 (1993); K. Vogel, W. P. Schleich, M. O. Scully, and H. Walther, *ibid.* **48**, 813 (1993); C. Wagner, R. J. Brecha, A. Schenzle, and H. Walther, *ibid.* **47**, 5068 (1993).